International Journal of Mass Spectrometry 392 (2015) 23–27

Contents lists available at ScienceDirect

International Journal of Mass Spectrometry

journal homepage: www.elsevier.com/locate/ijms

Electron detachment of NO^- in collisions with O_2 and N_2 below 10 keV

L. Serkovic-Loli [a], L. Hernández [a], E.M. Hernández [a,b], G. Hinojosa [a,*]

[a] Instituto de Ciencias Físicas, Universidad Nacional, Autónoma de México, A.P. 48-3, Cuernavaca 62251, Mexico
[b] Facultad de Ciencias, Universidad Autónoma del Estado de Morelos, Cuernavaca 62210, Mexico

ARTICLE INFO

Article history:
Received 12 June 2015
Received in revised form 21 August 2015
Accepted 21 August 2015
Available online 31 August 2015

Keywords:
Electron detachment
Molecular anions
Cross-sections
Thermal electrons

ABSTRACT

Measurements for the total electron detachment cross-sections with the beam attenuation technique and for the single electron detachment cross-sections with the growth rate method of NO^- in collisions with O_2 and N_2 are reported. Differences of one order of magnitude between the measuring techniques were found. Possible contributions of auto-detachment processes and an application of the geometrical model are discussed.

1. Introduction

Nitric oxide (NO) and its ions are ubiquitous in many gas phase plasmas, either as a dissociation by-product from NO_2 or as a residual gas in vacuum systems. After O^-, the nitroxyl anion (NO^-) is the most abundant anion in swarm measurements of NO_2-He mixtures [1]. It also appears as a result of electronic collisions with NO_2 [2]. The weakly attached electron in NO^- is a source of free thermal electrons that in film deposition plasma applications [3] may be the outset of electric breakdowns [4].

In cold plasma physics, the process of collision electron detachment (CED) from negatively charged species is a fundamental phenomenon. The ability to control the dielectric strength of gas mixtures depends on comprehending the relation of the effective electron detachment to the effective electron attachment coefficients [5].

NO^- has been used to benchmark electron affinity measurements by photodetachment [6–8] and by electron scattering techniques [9], and also in laser induced vibrational auto-detachment measurements [10]. In addition, ion mobility parameters of this particular anion have been studied in low temperature plasmas [1,11]. From a fundamental point of view, state-of-the-art quantum mechanical calculations [12] are still challenged to describe the physical processes that determine the stability of molecular anions. Despite its relevance in cold plasma and in fundamental physics, to our knowledge, no attempt to measure the collisional electronic detachment cross-section has been made for this archetypical anion.

In this paper, we offer a study based on measurements of the collisional detachment cross-section of NO^- on O_2 and N_2 gases below 10 keV kinetic collision energy.

2. Experiment

The experimental method consists in generating a beam of NO^- that passes through a gas-cell filled with either O_2 and N_2 high purity gases. The pressure in the gas-cell was maintained low enough for the signal to be proportional to the gas-cell pressure and high enough to get a good signal. As a result of the interaction, the negative NO^- ions (*parent ion beam*) may loose electrons or dissociate. The resulting neutral molecules or fragments were counted and the cross-section was derived from the intensities of the ion beam and the resulting neutral molecules and fragments count-rate as a function of the gas target density (π) in the gas-cell. Descriptions of the present experiment are also given in references [13,14]. Here we provide a description with more details that are relevant to the present experiment.

This study was carried out using an electrostatic accelerator designed to operate at kinetic energies below 10 keV; a schematic drawing is shown in Fig. 1. The ion beam of NO^- was produced by injecting a mixture of three parts per million of NO_2 in N_2 into the ion source chamber and kept at constant flux pressure. The ion source assembly was acceleration voltage-biased such that the negative ions produced inside were repelled to an Einzel lens set. These negative ions were mass separated by a magnetic field perpendicular to the ions' trajectory. Small adjustments in the trajectory of

* Corresponding author.
E-mail address: hinojosa@fis.unam.mx (G. Hinojosa).

http://dx.doi.org/10.1016/j.ijms.2015.08.020
1387-3806/

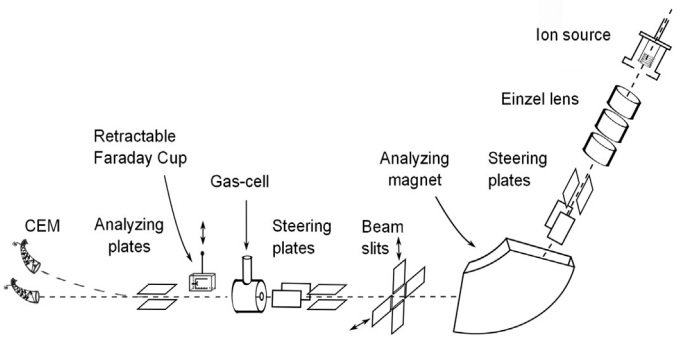

Fig. 1. Schematic drawing of the electrostatic accelerator taken from reference [14].

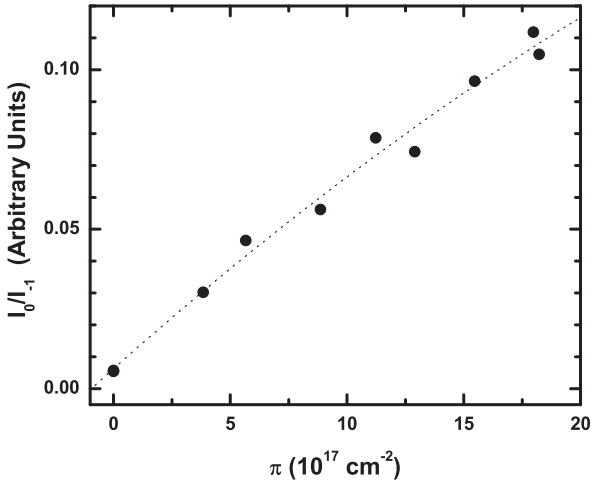

Fig. 2. Example of a signal growth rate curve for $NO^- + O_2 \rightarrow NO^* + O_2^* + e^-$. The dotted line represents a second order minimum square fit of Eq. (3) to the data. This example corresponds to 5 keV kinetic energy.

the ion beam were performed with the aid of two sets of voltage-biased parallel plates with electric fields perpendicular to the beam trajectory (steering plates in Fig. 1). The input and output collimator orifices in the gas-cell had diameters of 1.0 mm and 1.5 mm respectively. Finally, a set of $x-y$ linear motion slits placed after the analyzing magnet were used to control the ion beam width and to monitor its profile. The ion beam width was typically 0.5 mm.

The neutral molecules and fragments resulting from collisions in the gas-cell were separated from the parent ion beam by a perpendicular electric field (analyzing plates in Fig. 1) that was also used to direct ions to a channel electron multiplier (CEM) located in one side of the accelerator axis. Neutral molecules and fragments were detected and counted with an identical CEM facing the axis of the accelerator.

To check the collection efficiency of the fragments and neutral particles by the CEM detectors, tests that recorded the parent ion beam intensity and charged fragments after being scattered as a function of the electric field in the analyzing plates were performed. These tests systematically exhibited an intensity plateau, thereby showing that the resulting particles spread were smaller than the CEMs collection aperture after dispersion in the gas-cell. The CEMs aperture widths were 0.7 cm.

In the present experiments, it was important to operate the CEMs under similar gain and efficiency conditions. To verify these requirements, the counting rate in the central CEM was measured with analyzing plates electric field set to zero; this gives the overall count rate: neutral particles plus the negative parent ion beam. With the electric field on, the lateral CEM count rate corresponds to the parent ion beam; this count rate plus the central CEM count rate (neutral particles) were verified to be comparable to the central CEM total counting rate. This check was performed with the gas-cell empty. The CEMs bias voltage gains were also adjusted for maximum count rates.

The systematic uncertainties in this experiment arise mainly from the gas-cell pressure and temperature measurements that propagate a 10% systematic uncertainty to the cross-sections. The kinetic acceleration energy measurement has a maximum 5% uncertainty. The ion source assembly was located in a region where the base pressure was 8×10^{-4} Pa without gas load. With gas load, the operation pressure in this section of the accelerator was 5×10^{-2} Pa. The pressure in the detection chamber was 5×10^{-5} Pa. The pressure in the gas-cell was measured with an absolute calibrated Baratron.

To calibrate this experiment, we measured electron detachment cross-sections for collisions of H^- with O_2 in the energy range of 1 keV to 10 keV and compared to values by Allen et al. [15] who measured with an ionization gas-cell. We also measured well known electron capture cross-sections of protons on Ne and CH_4 in the energy range of 2 keV to 10 keV and compared with measurements by Kusakabe et al. [16], Allison [17], Rudd [18] and Lindsay et al. [19]. Our results were in agreement with these previous measurements.

To study the collisional electron detachment cross-section we chose two different techniques, the signal growth rate method (SGR) and the beam attenuation technique (BAT). The SGR method is based on the solutions to the equilibrium equations for the fraction of neutral particles to the number of anions in the ion beam F_0 as a function of the target density π. F_0 is derived from

$$F_0 = \frac{I_0 - I_b}{I_i} \tag{1}$$

where I_0 is the signal count rate of neutral particles resulting from the interaction with the gas, I_b and I_i are the signal count rates resulting from the interaction with the vacuum residual gas and ions in the parent ion beam respectively. π is defined as

$$\pi = \frac{\ell P}{\kappa T} \tag{2}$$

where ℓ is effective length, P the pressure and T the temperature of the gas-cell. κ is Boltzman's constant.

The SGR method is described in a more detailed manner in references [13,15,20]. In this method it is assumed that the fraction F_0 of neutral particles formed after the ion beam looses an electron by collisions with the gas is a function of the initial parent ion beam intensity and the target density. In the present case, we have derived the single detachment cross-section σ_{-10} from the second order approximation to F_0

$$F_0 = \sigma_{-10}\pi + \xi\pi^2, \tag{3}$$

where σ_{-10} is the single collision detachment cross-section and π the target density. ξ accounts for product contributions to F_0 from other processes such as double electronic detachment ($\sigma_{-10}\sigma_{-11}$) and fragmentation when the parent ion beam can be considered as composed of only one charge state, as in the present case.

An example of a growth rate curve of the present data is shown in Fig. 2. To check the second order correction contribution, we derived additional SGR cross-sections from first order fits to the F_0 versus π in a much lower gas-cell pressure regime (linear) for a set of selected cases and compared them with the present second order fits as given by Eq. (3). Systematically, cross-sections derived from second order corrected fits were higher; the difference between the two approaches accounted for an average of 20% in the case of the O_2 target and for an average of 10% in the case of N_2 target.